Large eddy Simulation of Flame Acceleration and Transition from Deflagration to Detonation

Cheng Wang[1*], Yongyao Zhao[1],Wenhu Han[2]
[1]State Key Laboratory of Explosion Science and Technology, Beijing Institute of Technology, Beijing 100081, China
[2] Center for Combustion Energy, Tsinghua University, Beijing 100084, China

1 Introduction

The 5-th order weighted essentially non-oscillatory (WENO) [1] finite difference scheme is combined with the large eddy simulation (LES) method to simulate flame acceleration and transition from deflagration to detonation in different width channels. The LES equations are obtained by filtering the compressible Navier-Stokes equations used a spatial filter based on the local grid size, which contain mass, momentum, total energy and mass fraction of reactant conservation equations. In order to close the unclosed quantities in the equations, a transport model for the sub-grid kinetic energy and the dynamically thickened-flame (TF) combustion model are used [2,3]. In the TF model, the flame front is artificially thickened to be resolved on LES mesh, which is simply achieved by decreasing the pre-exponential factor of the chemical Arrhenius law whereas the molecular diffusion is enhanced by a factor F . The response of the thickened-flame to turbulence is considered by incorporating an efficiency function [4] in the governing equations. The flame acceleration and DDT of ethylene-air premixed mixture are simulated in different width channels with no-slip and adiabatic walls. The goal of this work is to investigate the effect of the width on the DDT process and the detonation mode by LES method.

2 Governing equations

The governing equations are obtained by filtering the compressible instantaneous conservation Navier-Stokes equations for mass, momentum, total energy and species conservation. The equations are as following:

$$\frac{\partial \bar{\rho}}{\partial t}+\frac{\partial}{\partial x_i}(\bar{\rho}\tilde{u}_i)=0 \tag{1}$$

$$\frac{\partial \bar{\rho}\tilde{u}_i}{\partial t}+\frac{\partial}{\partial x_i}(\bar{\rho}\tilde{u}_i\tilde{u}_j+\bar{P}\delta_{ij})=\frac{\partial}{\partial x_i}(\tilde{\tau}_{ij})-\frac{\partial}{\partial x_i}(\tau_{ij}^{sgs}) \tag{2}$$

$$\frac{\partial \bar{\rho}\tilde{E}}{\partial t}+\frac{\partial}{\partial x_i}((\bar{\rho}\tilde{E}+\bar{P})\tilde{u}_i)=\frac{\partial}{\partial x_i}(\tilde{u}_i\tilde{\tau}_{ij})-\frac{\partial \bar{q}_i}{\partial x_i}-\frac{\partial}{\partial x_i}H_i^{sgs} \tag{3}$$

Correspondence to: wangcheng@bit.edu.cn

$$\frac{\partial \overline{\rho}\tilde{Y}}{\partial t}+\frac{\partial}{\partial x_i}\overline{\rho}\tilde{Y}\tilde{u}_i=\frac{\partial}{\partial x_i}(\overline{\rho}F\xi D_i\frac{\partial \tilde{Y}}{\partial x_i})-\frac{\partial}{\partial x_i}\varphi_i^{sgs}+\frac{\xi\dot{\overline{\omega}}}{F} \tag{4}$$

$$\frac{\partial \overline{\rho}k^{sgs}}{\partial t}+\frac{\partial}{\partial x_i}(\overline{\rho}\tilde{u}_i k^{sgs})=\frac{\partial}{\partial x_i}(\overline{\rho}\frac{\upsilon_t}{pr}\frac{\partial k^{sgs}}{\partial x_i})-\tau_{ij}^{sgs}(\frac{\partial \tilde{u}_i}{\partial x_j})-C_e\overline{\rho}(k)^{3/2}/\Delta \tag{5}$$

The overbar means spatial filter, for a flow variable f , its filtered quantity denoted as

$$\overline{f}(x)=\int f(x')F(x-x')dx' \tag{6}$$

In the equations, the Favre averaging is defined by $\tilde{f}=\overline{\rho f}/\overline{\rho}$. Here ρ , u , P , τ , E , q , Y , $\dot{\overline{\omega}}$ and k^{sgs} denote density, velocity, pressure, stress, total energy, energy diffusion vector, mass fraction, filtered reaction rates and sub-grid-scale (SGS) kinetic energy, respectively. The gradient method is used for the closure of the unclosed quantities. The sub-grid stress τ_{ij}^{sgs} , the unclosed term H_i^{sgs} in the energy equation and sub-grid diffusion of specie mass fraction are closed as

$$\tau_{ij}^{sgs}=-2\overline{\rho}\upsilon_t(\tilde{s}_{ij}-\frac{1}{3}\tilde{s}_{ij}\delta_{ij})+\frac{2}{3}\overline{\rho}k^{sgs}\delta_{ij} \tag{7}$$

$$H_i^{sgs}=-\overline{\rho}\frac{\upsilon_t}{pr_t}\frac{\partial \tilde{h}}{\partial x_i} \tag{8}$$

$$\varphi_i^{sgs}=-\overline{\rho}\frac{\upsilon_t}{Sc_t}\frac{\partial Y}{\partial x_i} \tag{9}$$

Here $\upsilon_t=C_\upsilon(k^{sgs})^{1/2}\Delta$, h denote total enthalpy, and $h=E+P/\rho$. The sub-grid reaction rates in the chemical source term are closed as

$$\dot{\overline{\omega}}=A\overline{\rho}\tilde{Y}exp(-\frac{Ea}{R\overline{T}}) \tag{10}$$

This model assumes perfect mixing at the SGS level and neglects SGS fluctuations. The expression implicitly assumes that the turbulent subgrid time scale is short than all chemical time scales. The thickening factor is defined as $F=1+(F_0-1)\Omega$, where F_0 is set to $max(N\Delta/\delta_L,1)$, N is the grid number in the flame front, Δ is the cell size and δ_L is the thickness of laminar flame, and the flame sensor is $\Omega=16[Y(1-Y)]^2$. The efficiency factor ξ is evaluated using a power-law flame wrinkling model that assumes the internal structure of the flame is not significantly altered by turbulence[4]. Constant values of 0.067 and 0.916 are employed for model coefficients C_υ and C_e , pr_t and Sc_t are taken to be 1.0 in the LES equations.

3 Results and discussions

First, we simulated the experiment [5] in tube with inner width 1 mm to test the validation of our model. A two-dimensional model is established, and the computational domain is 1mm × 1.22m, which filled with stoichiometric premixed ethylene-oxygen, the upper and bottom wall are non-slip solid. We set a high-temperature region with T=2250K in the middle of the computational domain to realize weak ignition. Fig. 1 shows the velocity evolution of the flame tip, the solid line with squares represents the experimental value, and the other represents numerical value. In experiment, the flame in the tube experience a long time acceleration period accelerates before reaching the maximum value 2700m/s then propagates at approximately 2300m/s. The numerical value provides agreement with the experimental velocity, the flame first accelerates, at t=0.19ms reaches the maximum value 2800m/s，which is late 0.01ms than the experiment，and the value is greater 3.7%. The detonation velocity is

2490m/s, which is also close to the theoretical detonation speed for stoichiometric ethylene-oxygen mixture.

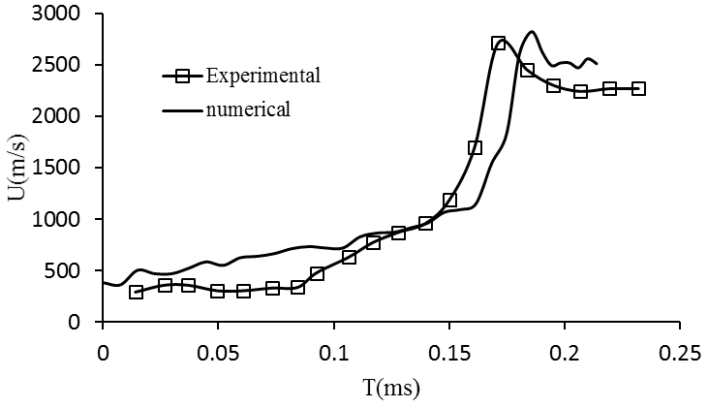

Fig. 1 Velocity evolution of the flame tip of experimental and calculated

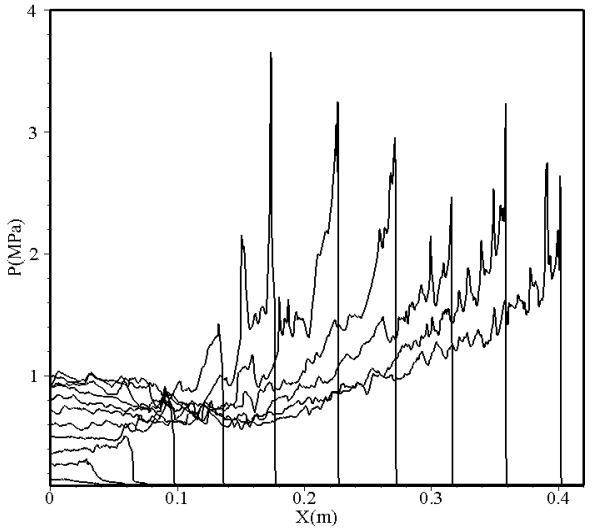

(a)

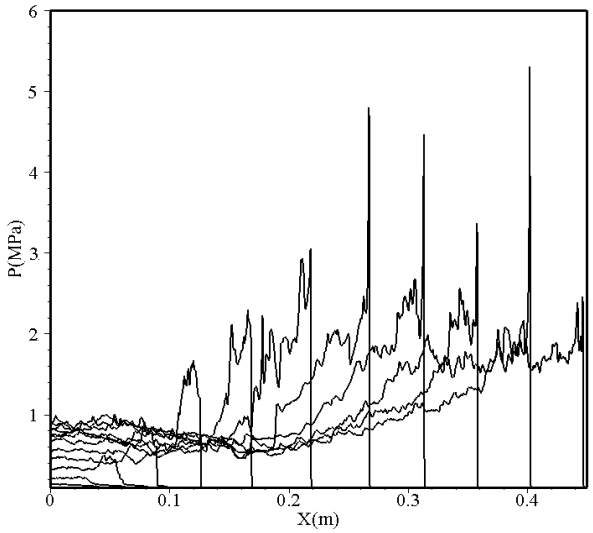

(b)

Fig.2 Evolution of pressure profile in different channels at axis line (a) D=10mm, (b) D=20mm.

Then, we simulate flame acceleration of ethylene-air in different width channels to reveal the effect of the width on the DDT process and the detonation mode. Take two channels with width of 10mm and 20mm, and the length of the channel is 0.8m which filled by premixed mixture. In order to

simplify the issue, two-dimensional LES equations also are used. The computational domains are closed at the left end and open at the other end, and the wall of channels are no-slip and adiabatic. In the unreacted mixture, initial velocity, temperature and pressure are 0.0m/s, 300K and 1atm respectively. The expansion ratio is 7.5. We mesh the computational domain using uniform grid equaling to 0.02mm, and a planar flame by weak ignition is set at the left end.

Fig. 2 shows the pressure distribution along propagating direction at axis line for 10mm and 20mm channel. From the evolution of pressure profiles, it can be seen that in initial stage the pressure is low and close to the initial value in unreacted mixture in both 10mm and 20mm width channel. Hence, the flame in this stage can be considered as constant-pressure combustion. As the flame and the flow ahead of it accelerate, a strong discontinuity of the pressure can be formed and correspondingly leading shock appears. While the gradient mechanism of reaction can be formed and then the resulting pressure pulse develops into a sharp pressure peak. The formation of the gradient mechanism eventually leads to the onset of overdriven detonation which means DDT occurs. From fig. 2 it can be seen, when the width of the channel is 10mm, the DDT run-up distance is about 0.18m, while it is 0.27m for the 20mm channel. So flame propagates in wider channel need longer distance to transition to detonation.

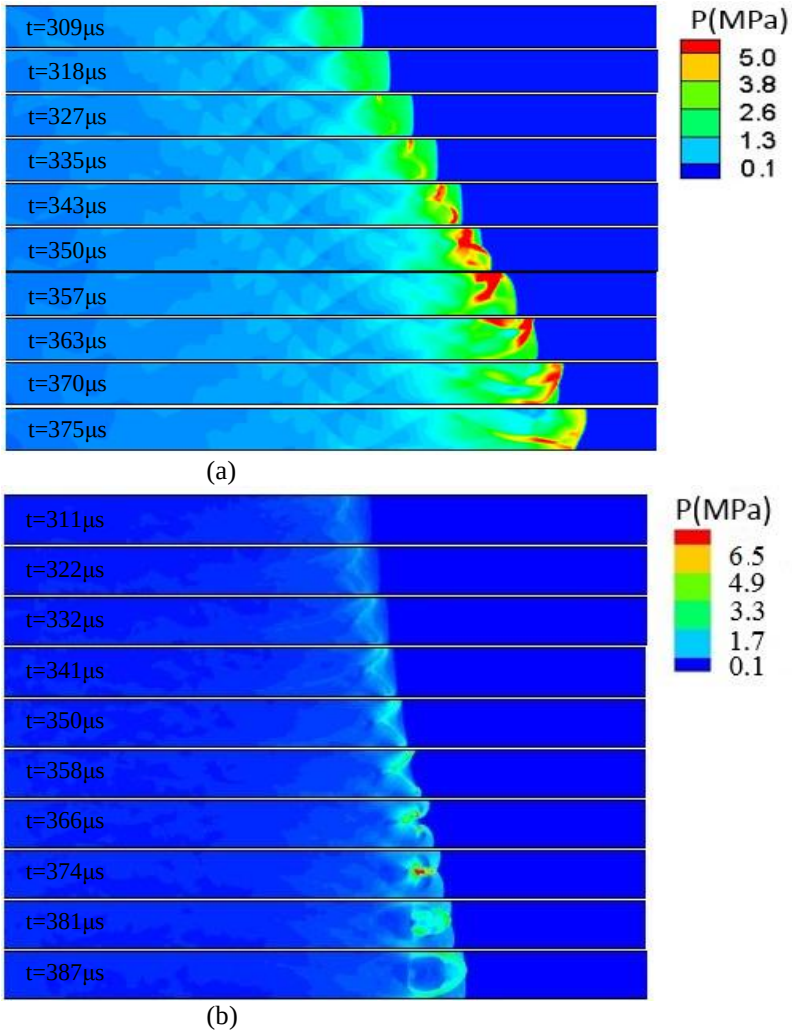

Fig. 3 Instantaneous pressure contours for transition to detonation (a) D=10mm, (b) D=20mm.

Fig. 3 shows the contours of the instantaneous pressure by the time sequence, and the evolution process of transition to detonation can be seen. When the channel width is 10mm, the effect of the boundary layer is significant on the transition to detonation. Hot spots with high pressure which are responsible for the local explosion form at the top wall (see fig. 3 (a)), then the transverse waves fully

develop and collide with the bottom wall, which induces the propagation of the detonation wave. Meanwhile, in the wider channel, the effect of layers will be less important in large width channels since the boundary layer is relatively thin compared to the channel width. Hot spots form at the center (see fig. 3 (b)) of the channel because of the collision of the reflected shock waves from top and bottom wall, which induces a local explosion.

The maximum pressure history can be considered as a recording of the tracks of detonation waves. Fig.4 illustrates the maximum pressure history for the case of D=10mm and 20mm channels. The channel width effects on the maximum pressure histories are plotted. The detonation cell size becomes regular with increasing channel width. Since there is no enough space in the small width channel to allow transverse mode appears, single head detonation forms after DDT and the single triple point collides constantly with the top and bottom wall and renders the detonation self-sustained. The cellular structure of the detonation recorded takes on a very regular quasi-periodic cellular structure, and this characteristic also is observed in the experiments and the simulations on the hydrodynamic structure of cellular detonation [6]. It is worth noting that, the detonation cell size of ethylene-air is approximately 19.5mm [7], so in the 10mm width channel, there are no whole detonation cell as the detonation waves propagating along the channel. However, in the wider channel, multi-head detonation can be formed and the cell is with many modes interacting nonlinearly. In our simulation, the cells size is not uniform, the smallest is less than 10mm, and the largest is close to 30mm. The experimentally measured data is in the range of our simulated values. It is interesting that the detonation waves reflected from the wall is not very clear, while the cell in the middle is regular. This shows that the viscous effect in boundary layer has obviously influence on the track of triple point in the transverse scale, but this seldom can be observed in the case of neglecting the viscous from the wall. The viscous heating layer may play key role in the formation of cell in the boundary; see [8] for further details.

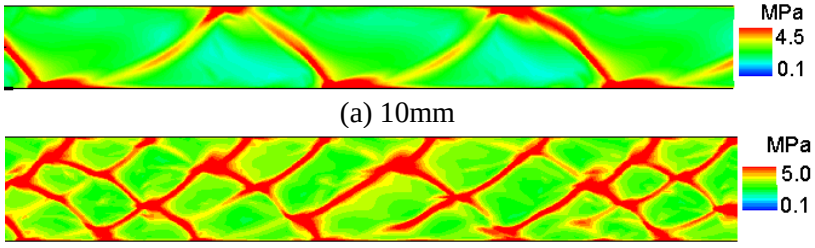

(a) 10mm

(b) 20mm

Fig.4 Maximum pressure history in different width channels

Acknowledgement

This research is supported by the Specialized Research Foundation for the Doctoral Program of Higher Education of China under grant number 20121101110004, Beijing Natural Science Foundation under grant number 8132034, and the Foundation of State Key Laboratory of Explosion Science and Technology under grant number ZDKT11–01.

References

[1] Jiang, GS, Shu CW. (1996). Efficient implementation of weighted ENO schemes. J. Comput. Phys. 126:202.

[2] Durand L, Polifke W. (2007). Implementation of the Thickened Flame Model for Large Eddy Simulation of Turbulent Premixed Combustion in a Commercial Solver. ASME Paper No. GT2007-28188.

[3] Colin O. (2000). A thickened flame model for large eddy simulation of turbulent premixed combustion. Phys. Fluids. Inst. 12: 7.

[4] Charlette, F., Meneveau, C., Veynante, D. (2002). A Power-Law Flame Wrinkling Model for LES of Premixed Turbulent Combustion Part I: Non-Dynamic Formulation and Initial Tests. Combust. Flame, 131, 159–180.

[5] Wu M.-hsun, Burke M.P., Son S.F., Yetter R.A., 2007. Flame acceleration and the transition to detonation of stoichiometric ethylene/oxygen in microscale channels. Proc. Combust. Inst. 31, 2429–2436.

[6] Radulescu MI, Sharpe G, Law CK, Lee JHS. (2007). The hydrodynamic structure of unstable cellular detonations. J.Fluid. Mech. 580:31.

[7] Sheldon R. Tieszen, Douglas W. Stamps, C. K. Westbrook, Willam J. Pitz, 1991. Gaseous hydrocarbon-air detonations, Combust. Flame, 84, 376-390.

[8] Valiev D, Bychkov V, Akkerman V, Eriksson c LE, Marklund M. (2008). Heating of the fuel mixture due to viscous stress ahead of accelerating flames in deflagration-to-detonation transition. Phys. Lett. A 372: 4850.